

Scissors modes in triaxial metal clusters

P.-G. Reinhard¹, V.O. Nesterenko^{1,2}, E. Suraud³, S. El Gammal⁴, and W. Kleinig^{2,5}

¹ *Institut für Theoretische Physik, Universität Erlangen, D-91058 Erlangen,*

Germany, E-mail: mpt218@theorie2.physik.uni-erlangen.de

² *Bogoliubov Laboratory of Theoretical Physics,*

Joint Institute for Nuclear Research 141980, Dubna,

Moscow Region, Russia, E-mail: nester@thsun1.jinr.ru

³ *Laboratoire de Physique Quantique, Université Paul Sabatier,*

118 Route de Narbonne, 31062 Toulouse, cedex,

⁴ *Physics Department, Faculty of Science,*

El-Menoufia University, Shebin El-Kom, Egypt

⁵ *Technische Universität Dresden, Institut für Analysis, Dresden, D-01062, Germany*

(Dated: October 29, 2018)

We study the scissors mode (orbital M1 excitations) in small Na clusters, triaxial metal clusters Na_{12} and Na_{16} and the close-to-spherical Na_9^+ , all described in DFT with detailed ionic background. The scissors modes built on spin-saturated ground and spin-polarized isomeric states are analyzed in virtue of both macroscopic collective and microscopic shell-model treatments. It is shown that the mutual destruction of Coulomb and the exchange-correlation parts of the residual interaction makes the collective shift small and the net effect can depend on details of the actual excited state. The crosstalk with dipole and spin-dipole modes is studied in detail. In particular, a strong crosstalk with spin-dipole negative-parity mode is found in the case of spin-polarized states. Triaxiality and ionic structure considerably complicate the scissors response, mainly at expense of stronger fragmentation of the strength. Nevertheless, even in these complicated cases the scissors mode is mainly determined by the global deformation. The detailed ionic structure destroys the spherical symmetry and can cause finite M1 response (transverse optical mode) even in clusters with zero global deformation. But its strength turns out to be much smaller than for the genuine scissors modes in deformed systems.

I. INTRODUCTION

The scissors mode in nuclei is a small-angle collective rotation of a *deformed* proton cloud against the complementing deformed neutron cloud. It thus belongs to the basic magnetic orbital dipole excitations. A rotation-like character of the mode assumes that it exists only in the systems with broken spherical symmetry. Early theoretical predictions are found in Refs. [1, 2] and its first experimental observation was reported in Ref. [3]. For a review see Ref. [4]. Since then, the scissors mode has also been discussed in other deformed systems, for example in quantum dots [5], Bose-Einstein condensates [6], and last not least in metal clusters [7, 8]. In the case of deformed metal clusters, the mode is viewed as a rotation-like collective oscillations of the electron cloud against the ionic background. There exist already a few theoretical considerations on that topic, early estimates from a collective perspective [7], RPA calculations with a phenomenological Woods-Saxon potential [8], and fully detailed RPA calculations using density-functional theory and jellium for the ionic background [9]. The relation of scissors modes to orbital magnetism had been discussed in Refs. [7, 8, 9, 10, 11]. Experimental access to scissors modes in clusters is yet an unresolved problem [12] (see also discussion in Ref. [9]). Nevertheless, or just because of that, further theoretical investigations are worthwhile in order to elucidate the nature of these modes and their key features.

It is the aim of this paper to present a theoretical investigation of scissors mode in Na clusters using time-dependent density functional theory for the electrons and fully detailed ionic background. We will consider in particular the triaxial clusters Na_{12} and Na_{16} . These two test cases provide several interesting features. As triaxial clusters, they have deformation in all three spatial directions and thus should display three distinct scissors modes. On the other hand, the single-particle excitation spectra are most diffuse in these soft systems which may give rise to strong fragmentation. Both clusters have spin-polarized and axially symmetric isomers which give rise to crosstalk with the spin-dipole mode which is energetically very close to the scissors mode. (The dipole and spin-dipole excitation spectra in Na_{12} had been studied extensively in Ref. [13].) The axial isomers allow also a direct comparison between scissors modes in axial versus triaxial shapes. We will investigate the impact of ionic structure on the scissors modes in two ways: first, we compare the triaxially deformed test cases with the results of the smooth jellium model, and second, we consider

as a complementing example the nearly spherical Na_9^+ with full ionic structure. The test case of axially symmetric Na_{11}^+ with jellium background is used to disentangle the various (counteracting) parts of the interaction, which compose the final prediction of the frequency of the mode.

II. FRAMEWORK

The electron cloud of the clusters is described by density-functional theory (DFT) at the level of the time-dependent local-density approximation (TDLDA) using actually the density functional of Ref. [14]. The coupling of ions to electrons is described by a local pseudo-potential which has been proven to yield correct ground state and optical excitation properties of simple sodium clusters [15]. The electronic wavefunctions are represented on an equidistant grid in three-dimensional coordinate space. The ground state solution is found by iterative relaxation. The time evolution is done by the time-splitting method. For details see the review [16].

To compute the spectral distributions, we employ spectral analysis after TDLDA propagation [16, 17]. This technique which had been developed and much applied for studying dipole resonances [16, 17, 18] is equally well adapted to the present case of the scissors mode. The dedicated initialization of the scissors channel is achieved by rotating the ground-state electron cloud by a small angle out of the equilibrium. The subsequent dynamics is analyzed with the orbital angular momentum $\langle \hat{L}_i \rangle$ which is the appropriate observable for the orbital M1 strength. Crosstalk between the principal axes of the cluster is very small. Thus rotation about the x -axis (using \hat{L}_x as a generator) explores the dynamics of $\bar{L}(t) = \langle \hat{L}_x \rangle$ and similarly for y and z . We follow the time evolution for 200 fs. The Fourier transform of $\bar{L}(t)$ provides the spectral strength distribution of orbital M1 strength. We also study the crosstalk to other modes. This is done simply by taking a protocol of the dipole moments $\hat{D}_i \propto r_i$ as well as spin-dipoles $S_i \propto r_i \hat{\sigma}_0$ (where $\hat{\sigma}_0$ is the Pauli spin matrix along quantization direction) and Fourier transforming them. In that case, we consider the spectral power distribution which is the sum of squared absolute values of the respective Fourier transforms. For a more detailed discussion of the spin-dipole see Ref. [13].

The global deformation of the cluster ionic background is crucial for the scissors excitations [7, 8]. It is characterized by the dimensionless quadrupole moments recoupled to the

total deformation β and triaxiality γ :

$$\beta = \sqrt{\beta_{20}^2 + 2\beta_{22}^2} \quad , \quad \gamma = \text{atan} \frac{\sqrt{2}\beta_{22}}{\beta_{20}} \quad ,$$

$$\beta_{2m} = \frac{4\pi}{5N_I} \frac{r^2 Y_{2m}}{r^2} \quad (1)$$

where N_I is the number of ions (atoms). The definition of the β_{2m} contains a simple classical averaging over the ionic positions.

In order to check the impact of ionic structure, we also use, as an alternative to the detailed ionic background, the soft jellium model [19] for the ionic density

$$\rho_I(\mathbf{r}) = \frac{\rho_{I0}}{1 + \exp((r - R(\Theta))/\alpha)} \quad , \quad (2)$$

$$R(\Theta) = R_0 \left(1 + \sum_{m=0,\pm 2} \delta_{2m} Y_{2m}(\Theta) \right) \quad (3)$$

where $R_0 = Cr_s N_I^{1/3}$, $r_s = 3.96 a_0$ is the Wigner-Seitz radius, the coefficient C is adjusted to ensure volume conservation $\int d\mathbf{r} \rho_i(\mathbf{r}) = N_I$, $\rho_{I0} = 3/(4\pi r_s^3)$ is the bulk density. The diffuseness α of the jellium surface allows to achieve a good reproduction of the empirical optical properties [19, 20]. It can be justified by folding a steep jellium drop with a local ionic pseudo-potential [19]. We choose the diffuseness $\alpha = 1 a_0$. The generating deformation parameters δ_{20} and $\delta_{22} = \delta_{2-2}$ are adjusted to give the intended deformations β and γ according to Eq. (1). The averaging in Eq. (1) then becomes a weighted integration over the jellium density ρ_I .

III. BASIC ASPECTS OF SCISSORS MODE

Before proceeding to the fully detailed TDLDA calculations, it is worthwhile to look at macroscopic features of the scissors mode as well as to present its simple microscopic view in terms of a deformed shell model.

A. Collective picture of rotational vibrations

In a collective picture, the scissors mode can be viewed as small-angle rotations of the spheroid of valence electrons against the spheroid of ions (see Fig. 1, part a)). More precisely, the displacement field of this mode consists out of a rigid rotation of the electrons

against the positive ionic background plus a compensating quadrupole term which serves to tune vanishing velocity at the surface [7] (see Fig. 1 , part b)).:

$$\vec{u}(\vec{r}) = \vec{\Omega} \times \vec{r} + \beta(1 + \beta/3)^{-1} \nabla(yz) \quad . \quad (4)$$

The distortion of the momentum Fermi sphere generates a restoring force leading to rotational oscillations which constitute the scissors mode [7].

The mode is characterized by low-energy oscillations with strong magnetic dipole transitions to the ground state. In axial clusters, the mode is specified by the states $|\Lambda^\pi = 1^+ \rangle$ where Λ is the projection of the orbital moment onto the symmetry axis z and π is the space parity. The corresponding energy and magnetic strength are [7, 8]

$$\omega_{M1} \simeq \frac{2}{r_s^2} N_e^{-1/3} \beta \quad (5)$$

$$\begin{aligned} B(M1) &= 4 \langle 1^+ | \hat{L}_x | 0 \rangle^2 \mu_b^2 \\ &= \frac{2}{3} \omega_{M1} N_e \overline{r^2} \mu_b^2 \\ &\simeq N_e^{4/3} \beta \mu_b^2 \end{aligned} \quad (6)$$

where N_e is the number of valence electrons (we use here natural units $m_e = \hbar = c = 1$). The value $B(M1)$ stands for summed strength of the degenerated x- and y-branches. The z-branch has vanishing strength for symmetry reasons. It is worth noting that $B(M1)$ does not depend on r_s and so is the same for different metals.

In triaxial clusters, the scissors mode splits into three branches with the frequencies [7]

$$\omega_{M1}^i = \omega_{M1} \begin{pmatrix} \cos \gamma + \frac{1}{\sqrt{3}} \sin \gamma \\ \cos \gamma - \frac{1}{\sqrt{3}} \sin \gamma \\ \frac{2}{\sqrt{3}} \sin \gamma \end{pmatrix} \quad (7)$$

and the strengths

$$\begin{aligned} B^i(M1) &= \frac{1}{3} \omega_{M1}^i N_e \overline{r^2} \mu_b^2 \\ &= \frac{1}{2} B(M1) \begin{pmatrix} \cos \gamma + \frac{1}{\sqrt{3}} \sin \gamma \\ \cos \gamma - \frac{1}{\sqrt{3}} \sin \gamma \\ \frac{2}{\sqrt{3}} \sin \gamma \end{pmatrix} \end{aligned} \quad (8)$$

where vectors run over $i = x, y, z$ components. The estimates show that both the frequencies and strengths are proportional to deformation β , which reflects the fact that collective

scissors modes can exist only in deformed systems. This feature may serve as an additional indicator of quadrupole deformation in clusters. The scissors mode has been already observed in several systems with different physical nature (nuclei, Bose condensate, quantum dots). This means that the mode is a general dynamical phenomenon persistent for deformed two-component systems. It is interesting to note that there is another kind of universal orbital magnetic mode, the twist M2 mode, which has been recently predicted in clusters [22]. The twist may exist in systems of any shape and it is the strongest multipole magnetic mode in medium and large *spherical* alkali metal clusters [22].

B. M1 transitions in the deformed shell model

In order to see which single electron states are the most relevant in building the scissors mode, we check the structure of the transition in the framework of the Clemenger-Nilsson model [23, 24]. The major shells \mathcal{N} of the spherical oscillator remain a useful sorting scheme for slightly deformed clusters. Taking into account that \mathcal{N} is connected with the space parity of the levels inside the shell as $\pi = (-1)^{\mathcal{N}}$, one may immediately conclude that $\Lambda^\pi = 1^+$ scissors mode has to be mainly generated by low-energy $\Delta\mathcal{N} = 0$ transitions inside the valence shell and high-energy $\Delta\mathcal{N} = 2$ transitions through two shells.

More information can be obtained from the expression for the orbital M1 transition element which in axially deformed clusters has the form

$$\begin{aligned} \langle \Psi_p | \hat{L}_{+1} | \Psi_h \rangle &= \frac{1}{2} \delta_{\pi_p, \pi_h} \delta_{\Lambda_p, \Lambda_h + 1} \\ &\sum_{nL} a_{nL}^p a_{nL}^h \sqrt{L(L+1) - \Lambda_h(\Lambda_h + 1)} \quad . \end{aligned} \quad (9)$$

Here, the wave function of a particle ($\nu = p$) or hole ($\nu = h$) deformed state $\Psi_{\nu=\mathcal{N}n_z\Lambda} = \sum_{nL} a_{nL}^\nu R_{nL}(r) Y_{L\Lambda}(\Omega) \chi_{1/2\nu}$ is written as a superposition of spherical (nL)-configurations in which n stands for the number of radial nodes; n_z labels the projection of the principle shell number $\mathcal{N} = n_x + n_y + n_z$ into z -axis. Eq. (9) shows that the scissors mode is generated by $\Lambda_p = \Lambda_h \pm 1$ transitions between wave function components belonging to one and the same spherical (nL)-configuration. In spherical systems ($nL\Lambda$)-states belonging to such configuration are degenerate while in deformed systems these states are energetically split and so may be connected by M1 transitions with non-zero energies. This is just the origin of the scissors mode. Obviously, the energy scale of the scissors mode is determined

by the deformation energy splitting and so is rather small. This explains predominantly low-energy ($\Delta\mathcal{N}=0$) character of the scissors mode. Just the low-energy branch exhausts most of the scissors $B(M1)$ strength. The high-energy ($\Delta\mathcal{N}=2$) branch of the mode carries much weaker strength since the particle states involved into ($\Delta\mathcal{N}=2$) transitions include only small fractions of (nL)-configurations from the valence shell.

One may show [8] that in the harmonic oscillator space the M1 transition matrix element is proportional to the matrix element of the quadrupole operator r^2Y_{21} . This indicates a coupling between the high-energy ($\Delta\mathcal{N}=2$) branch of scissors mode and electric $\lambda\mu = 21$ quadrupole plasmon in deformed clusters [8].

Note that in spherical clusters the M1 transitions connect degenerated states from one and the same (nL)-configuration. These transitions have zero energy and, therefore, the scissors mode in spherical *jellium* clusters is absent. The ionic structure destroys the spherical symmetry even at zero global deformation $\beta = 0$ and thus allows some $\hat{L}_{\pm 1}$ -response in such clusters. It remains to be seen how strong this effect is in actual calculations.

Eq. (9) hints that the strength of the scissors modes increases with the orbital moments L which are involved. Besides that, low azimuthal quantum numbers Λ favor the mode. In heavy clusters high orbital moments are accessible and thus these clusters can exhibit strong orbital effects [8]. Already at $N_e \sim 300$ the magnetic strength $B(M1)$ can reach impressive value of 300-400 μ_b^2 . The RPA calculations confirm the trend (5) for the frequency but reveal in light clusters considerable fluctuations around the trend (7) for the strength [8, 9]. These fluctuations are due to quantal shell effects. Finally, it is worth to mention that the scissors mode determines van Vleck paramagnetism and leads to strong anisotropy of orbital magnetic susceptibility [7, 8, 9, 10].

C. Preparatory example

As a first example, we consider the simple case of a strictly axial cluster. To this end we chose Na_{11}^+ with a soft jellium background (generating deformation $\delta_{20} = 0.38, \gamma = 0$). The symmetry allows only degenerate x - and y -scissors modes. The associated spherical valence shell (2s,1d) consists of 4 levels: $\mathcal{N}n_z\Lambda = 220, 211, 202$ and 200. In Na_{11}^+ , the Fermi level 220 is fully occupied and the other three levels remain empty. The only possible scissors transition is $220 \rightarrow 211$. The low density of particle-hole ($1ph$) excitations reduces fragmen-

tation of the M1 strength and thus one has only one pronounced scissors peak, the ideal scenario for a first exploration. The upper panel of Fig. 2 shows the spectral distribution of M1 strength. The full line is the result from the linearized TDLDA calculations [9, 21] with full interaction. We use this clean test case to identify the various contributions of the residual interaction. The ground state is always computed with the full energy functional. But for the excitation spectrum, we consider also the terms of the residual interaction separately. One finds in the upper panel the spectrum for the cases of no residual interaction at all (unperturbed $1ph$ response) and of pure Coulomb. The Coulomb interaction is strongly repulsive (like for the dipole mode) and results in a strong blue shift of the unperturbed strength. The blue shift for the total residual interaction is much smaller. This is due to the strongly attractive residual interaction from the exchange-correlation part of the functional. In fact, the exchange-correlation interaction alone produces so much attraction that the scissors mode acquires an imaginary frequency. The mode becomes unstable and is thus missing in the figure.

The lower panel of Fig. 2 shows as a complementing information the radial profile of the residual interaction. The density dependent operator $Q_{21}(\vec{r})$ of multipolarity $\lambda\mu = 21$ is in fact the (radially averaged) response potential $-(\partial^2 E/\partial\rho^2)\delta\rho$ where $\delta\rho$ is the transition density and E is the energy functional. The plot shows the full residual interaction as well as its two separate contributions. Repulsive parts are negative in this representation. One sees nicely that Coulomb is strongly repulsive, exchange-correlation is attractive and the total effect is a moderate repulsion. After all we see that the net residual interaction is composed from two counteracting pieces. This inhibits any general statement about the expected shift. Blue shift as well as red shift can emerge depending on the actual transition density. But one can predict that the total residual interaction will always be rather small (with possible exceptions in special cases).

IV. RESULTS AND DISCUSSION

A. Na_{12} : global deformation versus ionic structure

Figure 3 shows for Na_{12} the scissors strength, i.e. the Fourier transformed signal $\bar{L}_i(t)$, as computed from real time TDLDA (section II). The spin-saturated triaxial ground state

and spin-polarized axial isomer are considered with both ionic and jellium backgrounds. Triaxiality mixes the states with different Λ but still conserves the space parity. The ionic background makes the states parity mixed as well.

The spectra for the triaxial ground state (left lower panel) show the modes L_x , L_y , and L_z . The z -mode has one dominant peak at the low-energy end. Two other modes are strongly fragmented. A quick glance at the lower insert explains this. The density of $1ph$ states is very large in this neutral and triaxial cluster and thus spectral fragmentation is very likely. The lower end of the spectrum coincides with the lowest $1ph$ excitation which hints that the net effect of the residual interaction is rather weak. A simplified axial treatment can roughly explain the origin of three main peaks in x - and y -responses: in Na_{12} the Fermi level is one-half occupied level $\mathcal{N}_{n_z}\Lambda = 211$ and within the valence ($2s-1d$)- shell there should be three main scissors transitions: $220 \rightarrow 211$, $211 \rightarrow 202$, and $211 \rightarrow 200$.

Note also the M1 strength around 3 eV. This is the high-energy branch of the scissors mode. It emerges from the scissors transitions through two quantum shells ($\Delta\mathcal{N} = 2$) as mentioned in subsection III B. This branch exhibits a coupling to the $\lambda\mu = 21$ component of the quadrupole plasmon [8]. The energy range coincides perfectly with the position of the quadrupole plasmon around 3 eV (it is placed approximately at $\sqrt{6/5}$ times the frequency of the Mie plasmon which is here around 2.8 eV). The strength is strongly fragmented because the weakly bound triaxial Na_{12} has a high density of $1ph$ states in this energy region (actually not shown in the figure).

The upper left panel of Fig. 3 shows results for a comparable jellium background. For this aim, we have computed the global deformation of the ionic configuration. This yields $\beta = 0.55$ and $\gamma = 17^\circ$. The jellium background is tuned to have precisely the same deformation. The $1ph$ states start now at much lower energy since the energy gap at the Fermi surface is lower than with an explicit ionic configuration. This has two reasons: the jellium model is less bound here and we are not perfectly in the minimum of the jellium deformation energy surface, which does not coincide with the deformation associated to the case with explicit ions. Consequently, the whole spectra are shifted to lower frequencies where the first $1ph$ states are now situated. This corroborates again the fact that the residual interaction has a small effect. Moreover, we see by comparison with the $1ph$ spectra that the residual interaction can act both ways, repulsive or attractive. It is interesting to note that, in spite of the strong general downshift as compared to the case with detailed ionic background, the

relation amongst the scissors states (ordering, fragmentation) remains almost unchanged. And the downshift is simply given by the spectral gap in the ground state. This hints that global deformation is the crucial ingredient determining the pattern of the scissors spectra.

The comparison of the $1ph$ spectra in the left column of Fig. 3 is puzzling. It looks as if the better bound ionic configuration has the higher density of states. Part of this is indeed the effect that the larger spectral gap compresses the states just above the gap. Another part is generated by the fact that the jellium background is reflection symmetric about all three major planes while the ionic background induces slight symmetry breaking. There are more degeneracy in the jellium spectrum and none at all for the ionic background.

The right panels of Fig. 3 show the same analysis for the first isomer. This configuration is axially symmetric, i.e. $\gamma = 0^\circ$, but spin polarized with net spin 2 [13]. Total deformation is $\beta = 0.58$, close to the deformation of the triaxial state. The upper right panel (axial jellium model) shows nicely the exact degeneracy of x with y modes and the absence of the z mode. The spectrum is again fragmented in accordance with the high density of $1ph$ states. The lower right panel shows results with ionic structure. The z mode still nearly disappears. The degeneracy of x and y modes is somewhat broken because a detailed ionic structure breaks strict axial symmetry. This cluster is axial only in average, i.e. in the sense that $\gamma = 0^\circ$. The $1ph$ spectra are about at the same position in both cases here and similarly the fully coupled spectra. The responses are compatible with the assumption of small residual interaction. Moreover, we see that the detailed ionic structure does not help the z mode to show up (which would, in principle, be possible). Again, we conclude that global deformation determines the overall pattern of scissors modes.

The inserts between upper and lower panels in Fig. 3 show the collective estimates (7) and (5) for the scissors frequencies, obtained in a jellium model with given deformation parameters. Although the estimates belong to the jellium case, they can be connected with lower panels as well, as a collective view where only the global deformation counts. The estimates provide rough positions of the scissors modes but they miss any details. The actual spectra show that the details, driven by interference with $1ph$ structure, are crucial in these very soft clusters with a high level density.

B. Na₁₆: crosstalk

The orbital M1 mode and spin excitations belong to the same channel (see more on spin modes in clusters in Refs. [25]-[27]). The orbital strength $\sim B(M1) \propto N_e^{4/3}$ and power spectra $\sim B(M1)^2 \propto N_e^{8/3}$ evidently overrules the spin strength ($\propto N_e^0$) for large clusters. But they can compete in the small clusters considered here. There is an intriguing question how strong is a crosstalk between the modes. This point is better discussed in terms of power spectra, although we are in the linear regime. Mind that we are now plotting in logarithmic scale which is more appropriate for power spectra with their larger variations.

The various power spectra emerging from excitation of the scissors mode (i.e. with a rotational distortion) are shown for Na₁₆ in the upper block of Fig. 4 The block exhibits angular, spin-dipole and dipole responses. Both unpolarized ground state and spin-polarized first isomer of the cluster are considered. This case is different from Na₁₂ in that both configurations are triaxial. The spin-saturated ground state and spin-polarized isomer have deformations $\beta = 0.35$ with $\gamma = 38^\circ$ and $\beta = 0.32$ with $\gamma = 15^\circ$, respectively.

The uppermost panels show the angular momentum spectra associated with M1 strength. The patterns are similar to the previous case of Na₁₂ but differ in detail due to different $1ph$ distributions. The lowest panels of the upper blocks show the power spectrum in the dipole channel driven by the crosstalk with the angular momentum mode. The coupling is obviously very weak. In fact, there would be no crosstalk at all in a reflection symmetric jellium model. The effect here is triggered by the slight asymmetries in the detailed ionic configuration.

The middle panels show the crosstalk with the spin-dipole mode. There is no crosstalk at all in the case of the spin saturated ground state. But a strong crosstalk appears for the spin-polarized isomer. In that case, the scissors and spin motions are fully coupled and have to be considered as one hybrid mode. As complementing information, we show in the lower block of Fig. 4 the spin-dipole strength after spin-dipole excitation. For the isomer (right column), one recognizes the same spin-dipole spectrum as in middle panel of the upper block. The strength distribution is, of course, different because the excitation channel was different. For the spin saturated ground state (left column), there is now a clear spin-dipole signal. This mode is clearly separated from the scissors, but it resides precisely in the same low-energy range as the scissors mode. An experimental discrimination would require

to separate the spin and orbital currents. This question has been extensively discussed in nuclear physics where the form factor for inelastic electron scattering may give access to the separate information (see, e.g., Ref. [3]). The problem is much worse for clusters due to very low energies involved. The easiest way is to exploit the scaling with system size and to go for large clusters where spin-dipole excitations become relatively unimportant (see discussion in Ref. [9]).

It is worth to emphasize that the cross-talks discussed above connect the modes of the opposite space parity. This becomes possible due to mixing configurations of a different parity in the detailed ionic background.

C. Na_9^+ : pure ionic effects

As we have seen in the examples above, the scissors mode exists if the electron cloud can accomplish rotational-like oscillations against a massively deformed background. The mode does not work at all in the case of the perfect spherical symmetry. But clusters do have ionic structure which breaks spherical symmetry even if the global quadrupole deformation vanishes. It is then conceivable that the electron cloud performs rotational-like vibrations against the ionic background. Such transversal optical modes exist in the solid state [28]. Their frequency is proportional to momentum as in the acoustic branch. One may expect similar low-energy modes in a finite system with zero global deformation as well.

To check this, we consider the example of Na_9^+ . Its configuration consists in two rings of four ions topped by one single ion. The configuration has $\beta = 0.08$ and is thus fairly close to global spherical symmetry. It is to be noted that the top ion breaks reflection symmetry. Figure 5 shows the angular momentum strength in this cluster. There is some strength at 1.5-2 eV and another branch at 3.5-4.5 eV. The latter has position and strength much similar to the high-frequency branches in the previous examples. (The slight blue-shift is caused by positive net charge as compared to the neutral clusters considered before.) The branch is again related to the quadrupole plasmon and is predominantly composed of $\Delta\mathcal{N}=2$ transitions. However, the low-frequency branch has higher frequency and much weaker strength than in the previous examples. In fact it is related to $\Delta\mathcal{N}=1$ transitions. The larger frequency is explained by the fact that we deal here with a small magic cluster with a big HOMO-LUMO gap. The much lower strength is no surprise. Note that $\Delta\mathcal{N}=1$

transitions change space parity and would not be accessed by M1 motion in a jellium model. But the detailed ionic background mixes configurations of different parity and so even-parity \hat{L}_i operators can generate, though weak, the transitions of $\Delta\mathcal{N}=1$ kind. This explains why, unlike the previous examples, the first branch is weaker than the second one.

Such motion may be related to the transversal optical mode. But it is not possible to track that down unambiguously because in this small cluster the low-frequency M1 mode is predominantly of $1ph$ nature. Larger magic clusters are required for such an analysis. Altogether, we have seen magnetic M1 strength in a “spherical” cluster. This strength has different sources than the scissors mode. It takes place even at zero global deformation and has very little strength as compared to the genuine scissors modes.

V. CONCLUSIONS

We have presented fully microscopic TDLDA calculations for the scissors mode in small Na clusters taking into account detailed ionic structure, triaxiality and spin-polarization. The results were analyzed in terms of a simple collective (=macroscopic) picture and of more microscopic shell-model view of the mode. To single out the effects of ionic background, a comparison to jellium cases was done. Clusters with different global deformation (spherical, axial and triaxial) were considered.

The test case of Na_{11}^+ with jellium background displays straightforward and unfragmented scissors peak. This case was used to study the various contributions to the residual interaction defining the actual peak position. It revealed that Coulomb and exchange-correlation terms act in opposite directions, resulting finally only in a small collective energy shift. The actual sign depends on details, as e.g. interplay with particle-hole structures. The calculations for Na_{12} show that jellium results demonstrate good agreement with macroscopic estimates for the low-energy scissors branch, though the estimates miss such important aspect as fragmentation of the strength due to particle-hole states. There is also a high-energy scissors branch which is explained as a result of the transitions through two quantum shells.

Triaxiality produces a richer picture. It gives rise to an additional L_z -scissors branch and to considerable increase of the fragmentation. Besides that, triaxiality combined with the delicate balance between Coulomb and exchange-correlation contributions can lead to both red and blue shifts in one and the same spectrum.

Detailed ionic structure leads to the blue-shift of the scissors mode as compared to jellium results. It also considerably enhances the fragmentation. The ionic background causes small parity-mixing which results in a crosstalk, although weak, between positive-parity scissors and negative-parity dipole excitations. This crosstalk takes place for both spin-saturated and spin-polarized states. Spin-polarized states demonstrate in addition a strong crosstalk of the scissors and spin-dipole modes, the effect which is absent in spin-saturated states. Both modes happen to reside in the same corner of low-energy states which makes their experimental discrimination extremely tough.

Comparison of results from jellium with those using detailed ionic background shows that the scissors modes are mainly determined by the global deformation. The ionic background as such destroys locally the spherical symmetry and gives rise to some M1 orbital strength (as the transversal optical modes in solids). This becomes apparent by the existence of L_i response even in clusters with *zero* global deformation, like Na_9^+ . The strength of such a mode is an order of magnitude smaller than the collective scissors strength which lives up in truly deformed systems.

The scissors mode is a general dynamical effect peculiar to different Fermi (and even Bose) systems with a disturbed symmetry. In the particular case of atomic clusters, the mode demonstrates very interesting features deserving further study. The main problem, not tackled in this paper, is its unique experimental identification. Such questions will be considered in a forthcoming publication.

Acknowledgments

The work was supported by grants from RFBR (00-02-17194), Heisenberg-Landau program (BMBF-BLTP JINR), DFG (436RUS17/102/01) the French-German exchange program PROCOPE (99074), and Institut Universitaire de France. V.O.N. thanks N. Lo Iudice for useful discussions.

-
- [1] N. Lo Iudice and F. Palumbo, *Phys. Rev. Lett.* **41**, 1532 (1978).
 - [2] E. Lipparini and S. Stringari, *Phys. Lett.* **130B**, 139 (1983).
 - [3] D. Bohle *et al*, *Phys. Lett.* **B137**, 27 (1984).

- [4] N. Lo Iudice, *Prog. Part. Nucl. Phys.* **28**, 556 (1997).
- [5] Ll. Serra, A.Puente, and E. Lipparini, *Phys. Rev.*, **B20**, R13966 (1999).
- [6] D. Guéri and S. Stringari, *Phys. Rev. Lett.* **83**, 4452 (1999).
- [7] E. Lipparini and S. Stringari, *Phys. Rev. Lett.* **63**, 570 (1989); E. Lipparini and S. Stringari, *Z. Phys. D* **18**, 193 (1991).
- [8] V.O. Nesterenko, W. Kleinig, F.F. de Souza Cruz, and N. Lo Iudice, *Phys. Rev. Lett.* **83**, 57 (1999).
- [9] V.O. Nesterenko, W. Kleinig, P.-G. Reinhard, J.R. Marinelli, and F.F. de Souza Cruz, preprint 2002.
- [10] V.O. Nesterenko, W.Kleinig, F.F. de Souza Cruz, and J.R. Marinelli, in Proc. of Intern. Symposium on Cluster and Nanostructure Interfaces, Richmond, USA, 1999. Eds. P. Jena, S.N. Khanna and B.K. Rao, World Scientific, Singapour, 2000, p.209-216; Preprint JINR E4-2000-14, Dubna, 2000.
- [11] S. Frauendorf, V.V. Pashkevich and S.M. Reimann, *Surf. Review and Letters* **3**, 441 (1996).
- [12] H. Portales, E. Duval, L. Saviot, M. Fujii, M. Sumitomo, and S. Hayashi, *Phys. Rev.* **B63**, 233402 (2001).
- [13] C. Kohl, S.M. El-Gammal, F. Calvayrac, E. Suraud, P.-G. Reinhard, *Eur.Phys.Journ. D* **5**, 271 (1999).
- [14] O. Gunnarsson and B.I. Lundqvist, *Phys.Rev. B* **13**, 4274 (1976).
- [15] S. Kümmel, M. Brack, P.-G. Reinhard, *Euro. Phys. J. D* **9**, 149 (1999).
- [16] F. Calvayrac, P.-G. Reinhard, E. Suraud, and C. Ullrich, *Phys. Rep.* **337**, 493 (2000).
- [17] F. Calvayrac, P.-G. Reinhard, and E. Suraud, *Ann.Phys (N.Y.)* **255**, 125 (1997).
- [18] K. Yabana and G. F. Bertsch, *Phys. Rev.* **B54**, 4484 (1996).
- [19] P.-G. Reinhard, O. Genzken, and M. Brack, *Ann. Physik (Leipzig)* **5**, 576 (1996).
- [20] A. Rubio, L.C. Balbas, and J.A. Alonso, *Z. Phys. D***19**, 93 (1991).
- [21] W. Kleinig, V.O. Nesterenko and P.-G. Reinhard, to be published in *Ann.Phys (N.Y.)*; arXiv: physics/0110057.
- [22] J.R. Marinelli, V. Nesterenko, F.F. de Souza-Cruz, W. Kleinig, and P.-G. Reinhard, *Phys. Rev. Lett.* **85**, 3141 (2000).
- [23] K. Clemenger, *Phys.Rev. B* **32**, 1359 (1985).
- [24] W.A. de Heer, *Rev.Mod.Phys.* **65**, 611 (1993).

- [25] Ll. Serra et al, Phys.Rev. A **47**, R1601 (1993).
- [26] L. Mornas, L. Calvayrac, E. Suraud, and P.-G. Reinhard, Z. Phys. D **38**, 73 (1996).
- [27] Ll. Serra and E. Lipparini, Z. Phys. D **42**, 227 (1997).
- [28] H. Ibach, H. Lüth, *Festkörperphysik*, ch. 9.4, (Springer, Berlin 1981).

Figure captions:

Figure 1: Macroscopic view of scissors mode [7]: a) rigid rotation, b) rotation within a rigid surface.

Figure 2: Scissors photo-absorption cross section (upper panel) and radial profile of residual interaction (lower panel) for Na_{11}^+ . Four cases are compared: no residual interaction at all (denoted ph, dashed line in upper panel), only Coulomb residual interaction (dotted lines), only exchange-correlation part of residual interaction (dashed line in lower panel), full residual interaction (full line). No scissors strength could be shown for the exchange-correlation part alone because in this case the residual interaction is so strongly attractive that an imaginary frequency emerges.

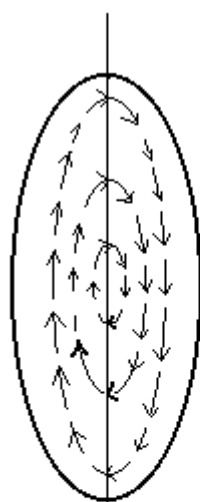
Figure 3: Strength distribution of angular momentum modes in Na_{12} . The quadrupole deformation of the jellium background is chosen to be the same as in the states with full ionic structure. The modes L_x , L_y , and L_z are distinguished by the lines as indicated in the left upper panel. Inserts under the panels show the 1ph spectra (bars) up to ~ 2 eV. The boxes in the left and right inserts between upper and lower panels show the collective estimates (7) and (5), respectively, for the scissors frequencies in the jellium model.

Figure 4: The upper block shows various power distributions in Na_{16} after angular excitation: angular (upper), spin-dipole (middle), dipole (lower). Unpolarized triaxial ground state (left) and spin-polarized axial isomer (right) are considered. The lowest block shows spin-dipole power following spin-dipole excitation. In all the calculations, full ionic structure is taken into account. Every case has three modes in each spatial direction. They are distinguished by lines as indicated.

Figure 5: Strength distribution of angular momentum modes in Na_9^+ , described with detailed ionic structure. The $1ph$ spectra at low energies are indicated in the insert below.



(a)



(b)

